Can Random Noise Injection Eliminate Noise?
Simulation and Hardware Implementation

Suleyman Kondakci
Faculty of Engineering & Computer Sciences, Izmir University of Economics, Izmir, Turkey

Keywords: Signal Reconstruction, Evoked Potentials, Semi–digital Signal Processing, Simulation, Implementation.

Abstract: Noise, found in all types of instrumentation and signal processing systems, has been a great challenge to tackle, especially, in biomedical signal processing tasks. Often, low-frequency and low power measurement signals are used in biomedical signal applications. This work is aimed at modeling and developing a simple, efficient, and inexpensive front end signal conditioner applying the cowpox approach to low-power analog signal measurements. We focus here on the simulation and implementation of a signal conditioner for the evaluation of its feasibility and efficiency based on the cost and accuracy constraints. As briefly outlined below, this article can serve as a model for facilitating the construction of semi–digital filters that can be applied to denoising of signals with low-frequency and very weak amplitude levels.

1 INTRODUCTION

This article presents a framework comprised of a concise theoretical background, simulations, optimization, and implementation of a novel semi–digital waveform denoising system that effectively enhances signal-to-noise ratio (SNR) of highly noisy measurements in real–time. The presented approach is based on the idea of *cowpox vaccination* combined with a recursive filtering technique. In order to validate the underlying method, we have built and evaluated an experimental filter, which mainly decomposes the noise–corrupted waveforms into a large number of analog samples, generates random noise samples, and injects the noise samples into the noise–corrupted waveforms, and performs an an averaging process in a recursive manner. The results obtained from the implemented system comply with the results of computer simulations and the underlying theoretical method. Efficiency of the implemented system is optimized in terms of a desired noise reduction level, number of recursions (waveforms), number of samples per waveform, and input noise level. There, exist several methods for filtering the random noise in biomedical instrumentations, e.g., (Guo, 2011; Ostry, 2006a; Zerguine et al., 2011; Momot, 2009; Pal and Mitra, 2012; Kamavuako et al., 2009; Durand and Froment, 2001; Kadambe and Srinivasan, 2006), and (Sharma et al., 2010) are the sources amongst a number of them that suggest different techniques to tackle the problem. The uniqueness of our approach lies in the modeling of the entire process, which uses *cowpox vaccination* combined with an analog register to thwart random noise components in a signal in the real-time. The analog register is modeled as a charge–transfer device (CTD), which stores individual signal samples as charge units in the register, (Janesick, 2001; Pain and Fossum, 1991) and (Cain and Morling, 1977). CTD of the implemented system stores 1024 signal samples as charge units while they are being transferred (shifted) from cell to cell in order to avoid excessive leakage of the charges. Signal denoising is done by a synchronized cowpoxing and averaging technique during the charge transfer in a recursive manner. That is, samples of the noisy signal are mixed with random noise samples by a summation process, the output of the summation circulates through charge cells while being delivered to the output of the filter. The filter output also circulates recursively through additional cowpoxing and summation operations until the desired reduction level is achieved. The number of recursions can be preset at the beginning of filtering or it can be automatically determined by observing the mean value of the output signal whether the mean value has reached the stationary state.

1.1 Outline of the Paper

The remainder of this paper is organized as follows. Section 2 gives a brief review on some related work

Kondakci S..
Can Random Noise Injection Eliminate Noise? - Simulation and Hardware Implementation.
DOI: 10.5220/0005011906040611
In *Proceedings of the 11th International Conference on Informatics in Control, Automation and Robotics* (ICINCO-2014), pages 604-611
ISBN: 978-989-758-039-0

and Section 3 presents the fundamental theory describing the model, which is used as the main approach for the realization of the proposed system. Section 4 introduces the methods used for the design of experiments and simulations used throughout the paper. Section 5 deals with the system simulation and discusses the dynamics of the presented algorithm. Section 6 discusses the overall system efficiency and derives the parameters for an optimum noise reduction. Section 7 introduces the realized hardware and Section 8 concludes the paper.

2 RELATED WORK

There have recently been many attempts to remove random noise from various types of signals using statistical inference methods mostly based on wavelet statistical models and Bayesian estimation, (Sameni et al., 2007). A survey of theoretical and practical aspects of hardware implementation of wavelet–based denoising filters is presented in (Gavrincea et al., 2007). Traditional filter implementations deal with cutting of unwanted frequency components, typically using low–pass, high–pass, or band–pass filtering configurations. Since the frequency range of random noise covers the entire frequency bandwidth of the processed signal, using the conventional pass/cut–based filtering method will also cut and distort the desired signal while processing. The signal averaging technique is an ideal solution to this essential problem, which recovers signal while quickly averaging out random noise components.

The recursive semi-digital signal averaging (RSDA) technique presented here bears also some limitations compared to non–recursive or finite impulse response (FIR) filters. Mainly, it can introduce phase shifts cause also bandwidth limitations due to the existence of feedback structures. This characteristic can limit its applicability to measurements involving very high frequency signal reconstruction tasks. On the other hand, a non–recursive filter will generally use more memory and CPU resources for its applications, which makes its use difficult in real–time applications, and more costly as well. Though most medical signal measurements operate with narrow–band signals, narrow–band filtering is not considered by RSDA, however, (Choi and Cho, 2002) proposes a useful algorithm for the suppression of narrow-band interference in direct sequence spread spectrum systems, based on the open–loop adaptive IIR notch filtering.

The application of signal averaging techniques are relatively old but steadily shows up in different applications, algorithms, and modifications. For example, as early as, (Bogdanov, 1997) has presented a comparison of discrete and continuous average techniques applied to multi–component force transducers. Most statistical algorithms are CPU–intensive and require more memory usage. An algorithm for robust weighted averaging with automatic adjustment of insensitivity parameter is introduced in (Leski and Gacek, 2004), where also the ensemble averaging and weighted averaging techniques are discussed in some context. The weighted signal averaging method (Laciar and Jane, 2001), different from the sample–based averaging presented here, is also sensitive to the presence of outliers in the measurement data, however, it has to perform intensive computations in order to estimate the noise variance in all signal cycles.

Adaptive filtering, which has been a popular research field for decades, is suitable for the reconstruction of periodic signals with very low frequencies. Though its efficiency is mainly based on the recursive estimation of error–free denoising and signal tracking parameters (Tichavsky and Handel, 1995), an adaptive filter can be effective for batch processing, but relatively inefficient in real–time applications compared to the semi–digital averager presented here.

Often, adaptive filtering gives good performance in low–amplitude signal measurements, e.g., an adaptive scheme for ECG enhancement is presented in (Almenar and Albiol, 1999). Influence of low frequency noise in adaptive estimation using the LMS algorithm is discussed in (Brito et al., 2009). A relatively computation–intensive approach is presented in (Laguna et al., 1992). A noise–constrained least mean fourth adaptive algorithm focusing on the learning speed of the adaptive algorithm is discussed in a newer work (Zerguine et al., 2011). Approaches given in (Momot, 2009) deals with a comprehensive study of weighted averaging of electrocardiogram (ECG), which applies Bayesian inference to the analysis of filter performance. Regarding the electrocardiography, an alternative noise reduction algorithm used for rhythmic and multitrial biosignals is presented in (Celka et al., 2008).

Wavelet–based denoising using (soft) thresholding involves several steps (Donoho, 1995); (1) performing a linear forward wavelet transform of the noisy data, (2) obtaining and performing a soft thresholding of the wavelet coefficients where the threshold depends on the noise variance, and (3) the coefficients obtained from step (2) are then used to obtain the signal estimate for the reconstruction of the signal (linear inverse wavelet transform). Obviously, this

involves an excessive number of operations compared to the sample–based averager presented here. Though the wavelet–based methods have been relatively successful in denoising of biological signals (Prasad et al., 2008), RSDA offers cost–effective real–time solutions to signal reconstruction tasks compared to computationally intensive wavelet–based, digital IIR and FIR approaches.

3 CONCISE DESCRIPTION OF THE METHOD

In contrast to widely encountered approaches used for signal denoising, we use a straightforward averaging technique applying the cowpox approach. Therefore, the theory behind this technique is trivial and the implementation of an appropriate filter is quite uncomplicated. We find several research done for denoising and signal correction also applying statistical approaches, e.g., (Blanco-Velasco et al., 2008; Pal and Mitra, 2012; Kabir and Shahnaz, 2012). For example, (Blanco-Velasco et al., 2008) considers ECG signal denoising and baseline wander correction based on the empirical mode decomposition, which decompose a signal into a collection of AM–FM components. Other known approaches, such as Fourier and wavelet-based methods, use traditional data analysis methods that require some predefined preprocessing functions to represent the signal. However, the technique presented here is uncomplicated, requires no preprocessing, and especially efficient in real-time denoising of evoked potentials an signals with some periodicity.

In the next section we use array notation for representing the signal and noise samples, e.g., $\mathbf{S}[\,]$ and $\mathbf{RNG}[\,]$ arrays. For convenience, we will use here the vector notation to denote these quantities. The RSDA algorithm decomposes the real–time input signal into discrete samples represented in the form of time series consisting of the measurement signal components (**s**) and independent random noise (**n**) components. Thus, $M \times N$ noisy signal components are mixed to construct a column vector space of M waveforms consisting of N column vectors defined as

$$\mathbf{c}_1 = \begin{pmatrix} \mathbf{w}_{(1,1)} \\ \mathbf{w}_{(2,1)} \\ \vdots \\ \mathbf{w}_{(M,1)} \end{pmatrix}, \ldots, \mathbf{c}_N = \begin{pmatrix} \mathbf{w}_{(1,N)} \\ \mathbf{w}_{(2,N)} \\ \vdots \\ \mathbf{w}_{(M,N)} \end{pmatrix}. \quad (1)$$

Mean value of each column vector can be obtained as

$$\overline{\mathbf{C}} = \left\{ \overline{\mathbf{c}}_1 = \frac{1}{M} \sum_{r=1}^{M} \mathbf{w}_{(r,1)}, \ldots, \overline{\mathbf{c}}_N = \frac{1}{M} \sum_{r=1}^{M} \mathbf{w}_{(r,N)} \right\}, \quad (2)$$

where, r denotes the number of recursions, i.e., number of waveforms each with N samples. It is obvious that the average values $\overline{\mathbf{c}}_1, \ldots, \overline{\mathbf{c}}_N$ accomplish the mean value of M waveforms into a single waveform $\overline{\mathbf{C}}$, i.e., the wave sample space is now a column-wise average of the input waveforms

$$\overline{\mathbf{C}} = \{\overline{\mathbf{c}}_1, \overline{\mathbf{c}}_2, \ldots, \overline{\mathbf{c}}_N\}.$$

As also supported by the simulation results, the higher the number of waveforms the better denoising will be achieved. This idea complies with the *low of large numbers*, i.e., summing infinitely many large random numbers will tend to be zero, see also Borel's low of large numbers, (Wen, 1991). Similarly, with the cowpox approach here, we recursively add as many noise samples as possible to the noisy signal so that the noise samples from the original signal will be substantially reduced. The larger the number of repetitions, the better the approximation tends to be. It can be easily verified that the above averaging process can be expressed in terms of a recursive function

$$\overline{\mathbf{W}} = \left(\frac{1}{M} \sum_{r=1}^{M} \overline{\mathbf{W}}_{(r,n)} \right)_{n=1,2,\ldots,N}. \quad (3)$$

Where, $\overline{\mathbf{W}}_{(r,n)}$ denotes the average value of rth iteration of the input signals each having n samples, where n can be set to at least 256 or more (e.g., 8192), depending on the sampling frequency and the quality of denoising required.

4 TEST SETUP

In order to determine the major parameters needed for an adequate system implementation a detailed simulation and associated real-time experiments with the implemented prototype system have been performed. With the test diagram shown in Figure 1, two types of signals, ECG signals and stimuli responses of electrodermal measurements (i.e., skin conductance) were experimented together with a white noise source. Though we apply a special form of the averaging technique to mostly periodic signals, we find several distinctive approaches applied to different types of signals. The algorithm and source chosen for the generation of the random noise play an important role with the cowpox method. Although we can find several implementations of random noise generators, e.g., (Lee et al., 2006) and (Ostry, 2006b), we preferred using a very special method due to its strengths underlined below. Our random noise generator (RNG) generates a sequence of 24-bit real numbers with uniform distribution and highly independent outcomes in the

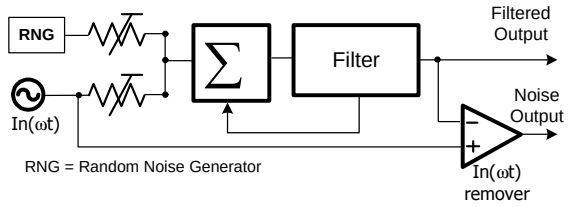

Figure 1: Diagram of the simulation and experiment setup, where RNG denotes the random noise generator and In(ωt) denotes the noisy measurement signal.

generated bit sequence. That is, the frequency of occurrence of each number in the sequence is approximately the same (uniformity), and no one value in the sequence can be inferred from the others (independence). Due to its strength and easy of implementation, we have used the Blum-Blum-Shub (BBS) algorithm, (Blum et al., 1986), which is claimed to be a cryptographically secure pseudo-random bit generator. Considering BBS as RNG for all practical purposes, the generated bit sequence is unpredictable (extremely random). The strength of such a pseudo-random number generator is such that given the first k bits of the sequence, there is no practical algorithm that can allow us to guess whether the next bit will be 0 or 1 with probability greater than $1/2$. Thus, the RNG unit (Figure 1) generates 24-bit random noise samples, which are further added to the noisy input signal sample-by-sample. For the simulation real–valued scalar quantities of clean input with a constant gain K and a noise signal were generated by

$$\mathbf{S}[\,] = K\ \sin\left(\frac{2\pi n}{N}\right), \quad n = 0,1,\ldots,N, \qquad (4)$$

and

$$\mathbf{RNG}[\,] = \mathsf{random}(\mathsf{SNR},\mathsf{N}); \quad -60 \le SNR \le 0, \ (5)$$

respectively. Arranging the generated bits in the array **byte**[ ] as a stream of 24-bit blocks (bytes each having 24 bits) and passing the bit blocks byte-by-byte through a 24–bit digital-to-analog (DAC) converter produces a relatively high–resolution analog data sample, which is stored in the random number generator array **RNG**[ ]. That is, **RNG**[ ] is now an array of N real numbers representing the noise samples. SNR denotes the signal–to–noise ratio in dB and N denotes the number of samples for both input and noise signals. As will be justified later, the higher the number of samples, the better the noise reduction can be achieved. Noisy input signal (**w**) to the averager is constructed as sample–by–sample addition of the elements of arrays **S**[ ] and **RNG**[ ]. The analog memory (CTD) used for the implementation of the filter has a charge leakage factor that can diminish the signal level. The leakage factor can have a great impact on the output if the number of recursions is extremely high. Hence, the instantaneous level (ith sample) of the signal measured at the output of the filter will correspond to

$$\mathcal{A} \times (\mathbf{W_i} + \mathbf{RNG_i}), \quad \mathcal{A} = e^{-\varepsilon r C_i \left(1-\cos\frac{2\pi}{C_i}\right)}, \qquad (6)$$

where r denotes the current recursion count, $\mathcal{A}$ denotes the overall transfer function of CTD having C memory cells, and ε stands for leakage factor for each cell. In order to achieve higher accuracy, the transfer function will be later (Section 5) modified with regard to both signal and sampling frequencies and the number of recursions as well.

5 SIMULATION

In order to determine parameters for an optimum resource usage (CPU time and memory) and for the selection of additional system components needed for the realization of the system, we have simulated the overall system with various configurations. In this concise version of the paper, we present only a brief formulation, related simulations, the implementation of the simulated system, and results of experiments with the implemented system. The simulation was first carried on with the straightforward addition of waveforms sample–by–sample

$$\mathbf{W}_{(r,n)} = \mathbf{W}_{(r-1,n)} + \mathbf{w}_{(r,n)}, \qquad (7)$$

which has gradually increased the amplitude of the sum with the increased number of iterations. Indeed, this approach constitutes the ”traditional averaging” technique invented several decades ago.

Obviously, increasing the number of recursions of ensemble averaging leads to instable outputs. Referring to the results from both simulations and real–time experiments, we have observed a significant level of saturation in the output signal. If, after each recursion, the output were scaled down by a certain factor, the output could be kept at a stable level. Hence, Eq. (7) has been experimentally modified to be

$$\mathbf{W}_{(r,n)} = \mathcal{A}\left[\mathbf{W}_{(r-1,n)} + \frac{\mathbf{w}_{(r,n)} - \mathbf{W}_{(r-1,n)}}{r}\right]. \qquad (8)$$

Actual system parameters such as gain and charge transfer leakage factor of the CTD used in the system implementation were also modified in order to match the simulation results. Most appropriately, the transfer function

$$\mathcal{A} = e^{-\varepsilon r C\left(1-\cos\frac{2\pi f}{fs}\right)}$$

describing both the gain and the leakage factor of the device chosen has been inserted into the averaging

function. Where, ε denotes the charge leakage factor, r number of recursions, C gives the number of charge cells, f and f_s depict the signal and sampling frequencies, respectively. Some results of the simulated experiments are shown both in Figure 2 and Figure 3.

6 EFFICIENCY AND OPTIMIZATION

We strictly aim at finding an optimum recursion count that minimizes the noise level to an acceptable level. Thus, it is important to determine the optimum number of recursions (i.e., processing power) needed to effectively reconstruct a noisy signal in terms of a desired reduction factor. Figure 2 (a) and (b) show the results from a simulated filtering process, whereas Figure 2 (c) depicts the noise reduction with respect to the number of recursions and Figure 2 (d) illustrates the mean value of the averaged signals at each iteration. The normalized noise reduction factor $\mathcal{R}$ can be parameterized as

$$\mathcal{R} \equiv f(\psi, r, N, K),$$

which can be further expressed in terms of *RMS* input–output ratio ψ combined with the number of samples per waveform (waveform size N) and the number of recursions r as

$$\mathcal{R} = \frac{\sqrt{\sum_{n=1}^{N} r\left[\overline{\mathbf{W}}_{(\mathbf{r},\mathbf{n})} - \overline{\mathbf{W}}_{(\mathbf{r-1},\mathbf{n})}\right] + \overline{\mathbf{W}}_{(\mathbf{r-1},\mathbf{n})}}}{r\sqrt{\sum_{n=1}^{N}\left(\overline{\mathbf{W}}_{(\mathbf{r},\mathbf{n})}\right)^{2}}}. \quad (9)$$

As depicted in Figure 2 (c), increase in the noise reduction is aligned with the theoretical description of the input–output ratio $\psi = RMS(In)/RMS(Out)$ and the current number of recursions r until the estimation parameters match the sample deviation and sample mean values, i.e., $\sigma^2 \approx 1$ and $\mu \approx 0$. The effect of the recursion count is illustrated in Figure 3, where a 512 sample extremely noisy input signal, Figure 3 (a), was denoised using 4096 recursions, Figure 3 (b). The evolution of the cumulative reduction in noise is shown in Figure 3 (c), and the corresponding RMS values of the filtered output at different recursion counts are shown in Figure 3 (d). These results comply with the theoretical analysis, which emphasize the fact that the amount of random noise will always tend to converge to zero with the increased amount of injected noise quantity along with the increased number of recursions. Figure 6 and 6 show other results from the implemented system, which has been tested with an extremely noisy sinusoidal stimulus applied to a skin admittance measurement.

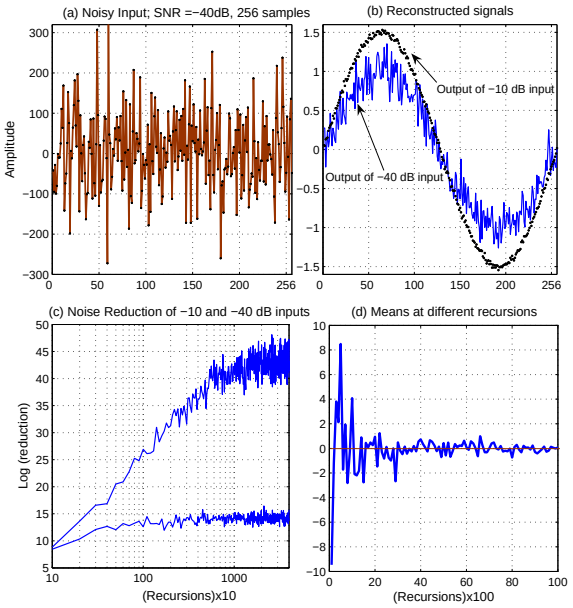

Figure 2: The tendency in the mean values and noise reduction of reconstructed waveform using 10.000 recursions: (a) Noisy input with -40dB SNR, (b) Filtered signals with -10dB and -40dB inputs, (c) Noise reduction versus recursions, (d) Mean values of filtered waveforms versus recursions.

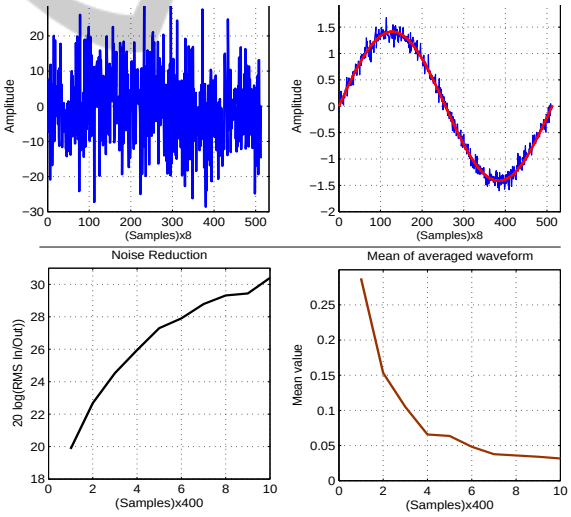

Figure 3: Effect of the injected white noise amount and the recursion count varying from 64 to 4096 iterations.

7 PROTOTYPE IMPLEMENTATION

We have designed and tested a relatively simple and effective semi-digital system. A simplified block diagram of the implemented system is shown in Figure

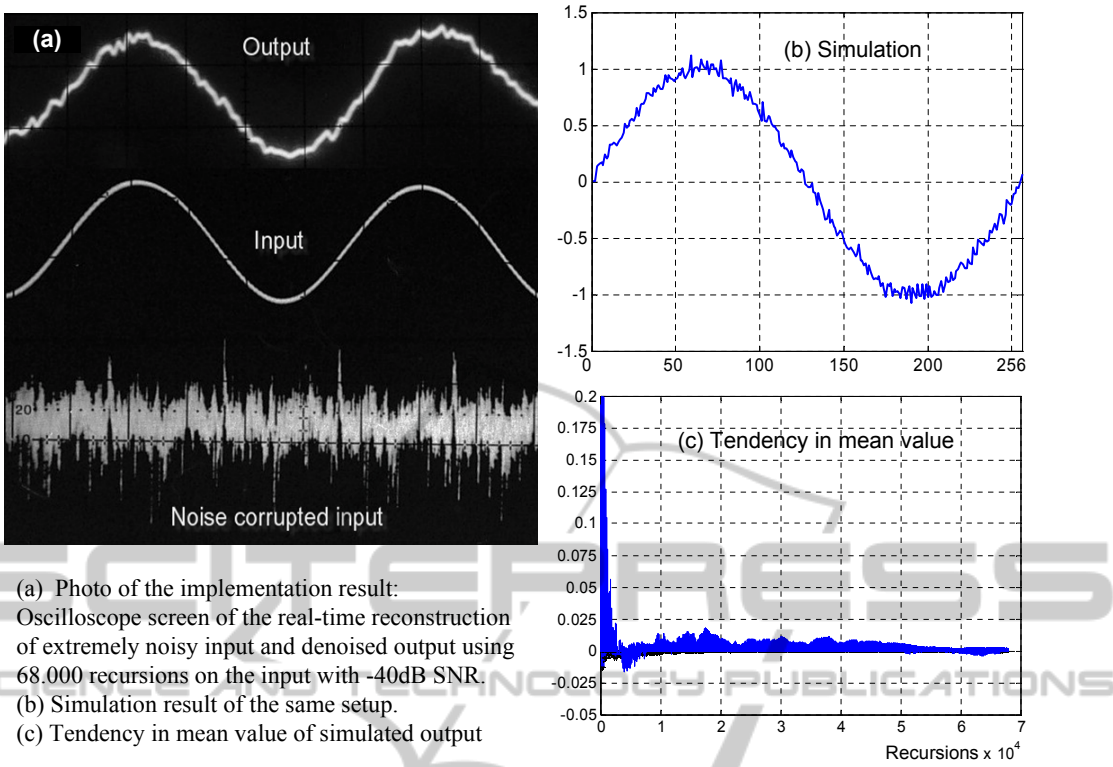

(a) Photo of the implementation result: Oscilloscope screen of the real-time reconstruction of extremely noisy input and denoised output using 68.000 recursions on the input with -40dB SNR.
(b) Simulation result of the same setup.
(c) Tendency in mean value of simulated output

Figure 6: Oscilloscope snapshot of noisy and clean inputs and outputs of an experiment and its simulation results.

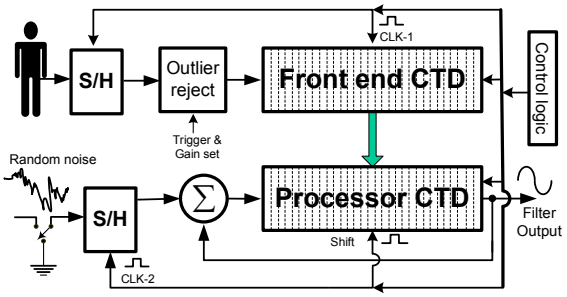

Figure 4: Block diagram of the prototype system.

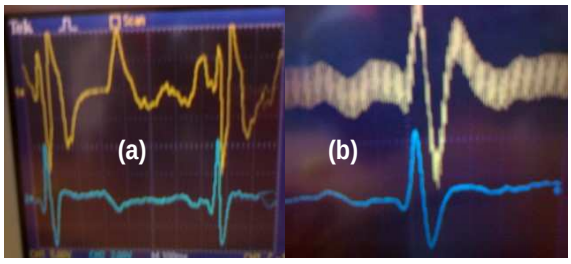

Figure 5: Construction of corrupted ECG signals, (a) with electrode motion artifact, (b) with addition of power-line signal.

4. Its hardware implementation contains two charge transfer devices (CTDs) each consisting of 1024 analog memory cells. The CTDs are bucket brigade device, (Scott and Chamberlain, 1980), type analog delay line circuits manufactured by EG & G Reticon ™. Results of an experiment with recording of a real–time electrocardiogram (ECG) is shown in Figure 5, where the first ECG signal was corrupted due to electrode motion artifacts and the second reading was superimposed by 50 Hz power-line signal.

8 CONCLUSIONS

In this article, we described a simple and efficient method for signal reconstruction covering simulations and design of a unique system that effectively enhances SNR in real–time. Basic theory of the proposed system is already known from before, however, the approach and the design described here are unique and efficient. Random noise injection into noisy measurements is the novelty of our approach not shown elsewhere. It is shown here that applying this approach (cowpox) to noisy signals followed by averaging process can perform a superior denoising, given that the noise of the input signal is also random. The results obtained from the simulations and real–time experiments comply with the associated theoretical analysis of signal averaging. Due to extensive resource usage, digital signal averaging

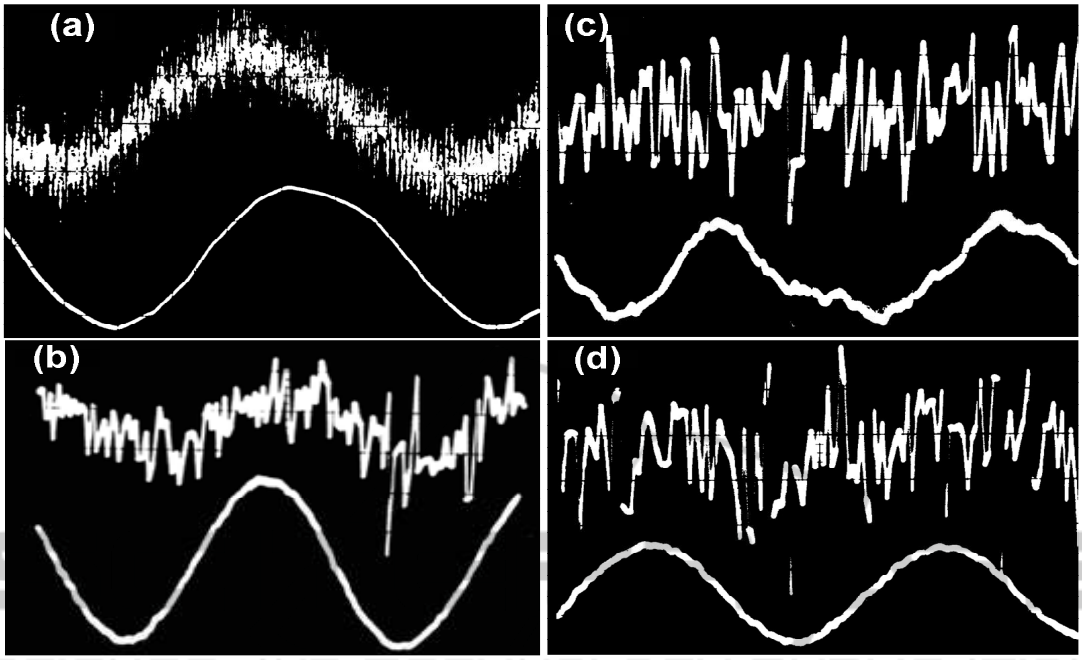

Figure 7: Oscilloscope snapshots of noisy inputs and denoised outputs.

technique is far more costly to implement compared to its semi–digital counterparts. The unique design presented here provides us a significantly inexpensive solution that can deal with noisy analog signals having very low frequency and amplitude ranges.

REFERENCES

Almenar, V. and Albiol, A. (1999). A new adaptive scheme for ecg enhancement. *Signal Process.*, 75(3):253–263.

Blanco-Velasco, M., Weng, B., and Barner, K. E. (2008). ECG signal denoising and baseline wander correction based on the empirical mode decomposition. *Computers in Biology and Medicine*, 38(1):1 – 13.

Blum, L., Blum, M., and Shub, M. (1986). A simple unpredictable pseudo random number generator. *SIAM J. Comput.*, 15(2):364–383.

Bogdanov, V. V. (1997). Comparison of the efficiency of averaging the signal from multicomponent force trans–ducers by direct and discrete methods. *MECHANICAL MEASUREMENTS*, 4(7):646–651.

Brito, D. S., Aguiar, E., Lucena, F., Freire, R. C. S., Yasuda, Y., and Barros, A. K. (2009). Fast communication: Influence of low frequency noise in adaptive estimation using the lms algorithm. *Signal Process.*, 89(5):933–940.

Cain, G. and Morling, R. (1977). C.C.D. processor for simultaneous time stretching and signal averaging. *Electronics Letters*, 13(9):269–270.

Celka, P., Le, K., and Cutmore, T. (2008). Noise reduction in rhythmic and multitrial biosignals with applications to event-related potentials. *Biomedical Engineering, IEEE Transactions on*, 55(7):1809–1821.

Choi, J. W. and Cho, N. I. (2002). Suppression of narrowband interference in ds-spread spectrum systems using adaptive iir notch filter. *Signal Process.*, 82(12):2003–2013.

Donoho, D. (1995). De-noising by soft-thresholding. *Information Theory, IEEE Transactions on*, 41(3):613–627.

Durand, S. and Froment, J. (2001). Artifact free signal denoising with wavelets. In *Acoustics, Speech, and Signal Processing, 2001. Proceedings. (ICASSP '01). 2001 IEEE International Conference on*, volume 6, pages 3685–3688 vol.6.

Gavrincea, G., Tisan, A., Buchman, A., and Oniga, S. (2007). Survey of wavelet based denoising filter design. In *Electronics Technology, 30th International Spring Seminar on*, pages 112–116.

Guo, H. (2011). A simple algorithm for fitting a gaussian function [dsp tips and tricks]. *Signal Processing Magazine, IEEE*, 28(5):134 –137.

Janesick, J. R. (2001). *Scientific Charge–coupled Devices*. SPIE Press Monograph Vol. PM83, Bellingham, Washington.

Kabir, M. A. and Shahnaz, C. (2012). Denoising of ECG signals based on noise reduction algorithms in EMD and wavelet domains. *Biomedical Signal Processing and Control*, 7(5):481 – 489.

Kadambe, S. and Srinivasan, P. (2006). Adaptive wavelets for signal classification and compression. {*AEU*} - *International Journal of Electronics and Communications*, 60(1):45 – 55.

Kamavuako, E. N., Yoshida, K., and Jensen, W. (2009). Variance-based signal conditioning technique: Com-

parison to a wavelet-based technique to improve spike detection in multiunit intrafascicular recordings. *Biomedical Signal Processing and Control*, 4(2):118 – 126.

Laciar, E. and Jane, R. (2001). An improved weighted signal averaging method for high-resolution ECG signals. *Computers in Cardiology 2001*, pages 69–72.

Laguna, P., Jane, R., Meste, O., Poon, P., Caminal, P., Rix, H., and Thakor, N. (1992). Adaptive filter for event-related bioelectric signals using an impulse correlated reference input: comparison with signal averaging techniques. *Biomedical Engineering, IEEE Transactions on*, 39(10):1032–1044.

Lee, D.-U., Villasenor, J., Luk, W., and Leong, P. (2006). A hardware gaussian noise generator using the box-muller method and its error analysis. *Computers, IEEE Transactions on*, 55(6):659 –671.

Leski, J. and Gacek, A. (2004). Computationally effective algorithm for robust weighted averaging. *Biomedical Engineering, IEEE Transactions on*, 51(7):1280–1284.

Momot, A. (2009). Methods of weighted averaging of ecg signals using bayesian inference and criterion function minimization. *Biomedical Signal Processing and Control*, 4(2):162 – 169.

Ostry, D. (2006a). Synthesis of accurate fractional Gaussian noise by filtering. *Information Theory, IEEE Transactions on*, 52(4):1609–1623.

Ostry, D. (2006b). Synthesis of accurate fractional gaussian noise by filtering. *Information Theory, IEEE Transactions on*, 52(4):1609 –1623.

Pain, B. and Fossum, E. (1991). Analog dynamic random-access memory (ADRAM) unit cell implemented using a CCD with feedback. *Electron Devices, IEEE Transactions on*, 38(1):178–179.

Pal, S. and Mitra, M. (2012). Empirical mode decomposition based ECG enhancement and QRS detection. *Computers in Biology and Medicine*, 42(1):83 – 92.

Prasad, V., Siddaiah, P., and Rao, B. (2008). Denoising of biological signals using different wavelet based methods and their comparison. *Asian Journal of Information Technology*, 7(4):146–149.

Sameni, R., Shamsollahi, M., Jutten, C., and Clifford, G. (2007). A nonlinear bayesian filtering framework for ECG denoising. *Biomedical Engineering, IEEE Transactions on*, 54(12):2172–2185.

Scott, D. and Chamberlain, S. G. (1980). Modeling and experimental simulation of the low-frequency transfer inefficiency in bucket-brigade devices. *Electron Devices, IEEE Transactions on*, 27(2):405–414.

Sharma, L., Dandapat, S., and Mahanta, A. (2010). Ecg signal denoising using higher order statistics in wavelet subbands. *Biomedical Signal Processing and Control*, 5(3):214 – 222.

Tichavsky, P. and Handel, P. (1995). Two algorithms for adaptive retrieval of slowly time-varying multiple cisoids in noise. *Signal Processing, IEEE Transactions on*, 43(5):1116–1127.

Wen, L. (1991). An analytic technique to prove borel's strong law of large numbers. *The American Mathematical Monthly*, 98(2):146–148.

Zerguine, A., Moinuddin, M., and Imam, S. A. A. (2011). A noise constrained least mean fourth (nclmf) adaptive algorithm. *Signal Process.*, 91:136–149.